15th World Congress on Computational Mechanics (WCCM-XV)
8th Asian Pacific Congress on Computational Mechanics (APCOM-VIII)
Virtual Congress: 31 July – 5 August 2022
S. Koshizuka (Ed.)

DEVELOPMENT OF TWO-PHASE FLOW SIMULATION USING SPH METHOD

MASAKAZU ICHIMIYA[1] AND NOBUKI YAMAGATA[2]

[1] The University of Tokyo
7-3-1 Hongo, Bunkyo-ku, Tokyo 113-8656 Japan
ichimiya.masakazu@gmail.com

[2]Advanced Creative Technology Co., Ltd.
2-10-3 Kojimachi, Chiyoda-ku, Tokyo102-0083, Japan
yamagata@actact.co.jp

Key words: Two-phase flow, WCSPH, Gas Entrainment, Die Cast, Filling Process

Abstract. *Gas entrainment is one of the major defects caused in the casting filling process. Since the particle method is a Lagrangian method that does not use a lattice, it can easily analyze large deformations and boundary movements, so it has the potential to be applied to gas defect prediction as a methodology. However, in the two-phase flow simulation including gas entrainment, the analysis fails when the gas / liquid density ratio becomes smaller than about 1/10 in the conventional SPH. Therefore, two dimensional two-phase flow SPH methodology was developed. Then, authors extended the methodology to three dimensions that can be applied to gas entrainent during a die cast filling process.*

1 INTRODUCTION

Gas entrainment is one of the major defects caused in the foundry filling process. Since the smoothed particle hydrodynamics (SPH) is a Lagrangian method that does not use a lattice, large deformations and movements can be easily analyzed, so it has the potential to be applied to such gas defect prediction as a methodology. However, numerical simulation of the two-phase flow, in particular those with large density ratio, has been challenging. It is because the discontinuities of the density and the sharp pressure gradient exist over the interface. Authors have developed a two-phase flow SPH methodology that can be applied to the foundry filling process containing gas.

The weakly compressible SPH(WCSPH) was used as the analysis method. Strictly speaking, water has a slight compressibility. The weak compressible SPH is solved by using NS equations and equations of state (EOS) alternately. The Tait equation was used for EOS.

The methodology developed in this study is applied to typical problems of gas-liquid two-phase flow including a dam break in air as well as a single bubble rising in water. The 2D as well as 3D bubble rising results show that both bubble shapes became similar to spheroids as shown by Grace. The water tests regarding the gas entrainment in the inclined part of the rectangular cavity and air exhaust from backstep part were also analized. Good agreement between the water tests and simulation results demonstrates the success of the SPH

methodology development.

The methodology in this study is applied to the 3D casting filling process simulation considering air entrainment.

2 TWO-PHASE FLOW SPH FORMULATION

2.1 Governing equations

The two-phase flow is considered in this study, and both phases obey the governing equations of a viscous Newtonian fluid.

$$\frac{D\rho}{Dt} = -\rho\nabla\cdot\boldsymbol{u} \quad (1)$$

$$\frac{D\boldsymbol{u}}{Dt} = -\frac{1}{\rho}\nabla p + \nu\nabla^2\boldsymbol{u} + \boldsymbol{g} + \boldsymbol{f} \quad (2)$$

ρ: density
$\boldsymbol{u}$: velocity vector
p: pressure
ν: kinematic viscosity coefficient
$\boldsymbol{g}$: gravity
$\boldsymbol{f}$: surface tension

Water has a slight compressibility and is strictly weakly compressible. The weakly compressible SPH method solves using NS equations and equations of state alternately. The following equation of state is used throughout this paper.

$$p = B\left[\left(\frac{\rho}{\rho_0}\right)^{\gamma} - 1\right] \quad (3)$$

Where, ρ_0 is reference density and B is as follows:

$$B = \frac{\rho {c_s}^2}{\gamma} \quad (4)$$

For water or liquid metals we use γ=7, and for gas γ=1 respectively.

The formulation used here is weakly compressible and is near the incompressible limit by choosing a sound speed c_s. Consequently the sound speed c_s, in the analysis, should be set about 10 times the maximum fluid velocity appearing in the analysis, not a physical value.

2.2 SPH formulation

The momentum equation (2) without gravity is discretized as follows;

$$\frac{Du_i}{Dt} = \frac{1}{m_i}\sum_j\left({V_i}^2 + {V_j}^2\right)\left[-p_{ij}\frac{\partial W}{\partial r_{ij}}e_{ij} + \mu_{ij}\frac{u_{ij}}{r_{ij}}\frac{\partial W}{\partial r_{ij}}\right] + f_i \quad (5)$$

Where

$$r_{ij} = \left|r_i - r_j\right| \quad (6)$$

$$V_i = \frac{m_i}{\rho_i} \quad (7)$$

Special treatment is needed for the interfaces of different phases. The density ρ is calculated by the following equation.

$$\rho_i = m_i\sum_j W_{ij} \quad (8)$$

Where m, W are mass and Kernel function respectively.

The pressure and viscous terms are approximated as follows[1]:

$$p_{ij} = \frac{(\rho_j p_i + \rho_i p_j)}{(\rho_i + \rho_j)} \quad (9)$$

$$\mu_{ij} = \frac{2\mu_i \mu_j}{(\mu_i + \mu_j)} \quad (10)$$

The following equation[2] is used for the surface tension term f.

$$f_i = -\frac{\sigma_i}{\rho_i} \kappa_i \frac{dc_i}{dx} \quad (11)$$

$$\frac{dc_i}{dx} = \frac{1}{V_i} \sum_j \left({V_i}^2 + {V_j}^2 \right) c_{ij} \frac{\partial W}{\partial r_{ij}} e_{ij} \quad (12)$$

$$\kappa_i = d \frac{\sum_j (n_i - \varphi_{ij} n_j) e_{ij} \frac{\partial W}{\partial r_{ij}} V_j}{\sum_j r_{ij} \frac{\partial W}{\partial r_{ij}} V_j} \quad (13)$$

Where d is the spatial dimension and $\varphi_{ij}$is defined as follows:

$$\varphi_i{}^j = \begin{matrix} -1 \ if\ particle\ i\ and\ j\ belongs\ to\ different\ phase \\ +1 \ if\ particle\ i\ and\ j\ belongs\ to\ same\ phase \end{matrix} \quad (14)$$

3 NUMERICAL RESULTS

3.1 2D Analysis of Dam Break in Air

The water column collapse was analyzed by changing the gas density. The calculation conditions are shown in Figure 3.1. The aspect ratio (H / L) of the water column was set to 2. The density ratios of gas and water were changed parametrically to 1/1000, 1/100 and 1/10.

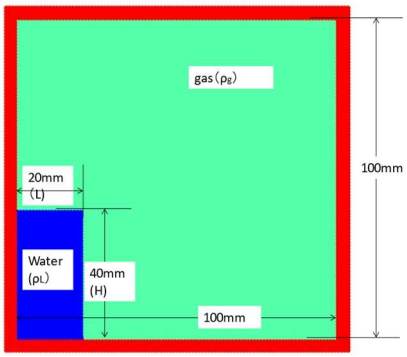

Figure 3.1 Calculation conditions for water column collapse in gas

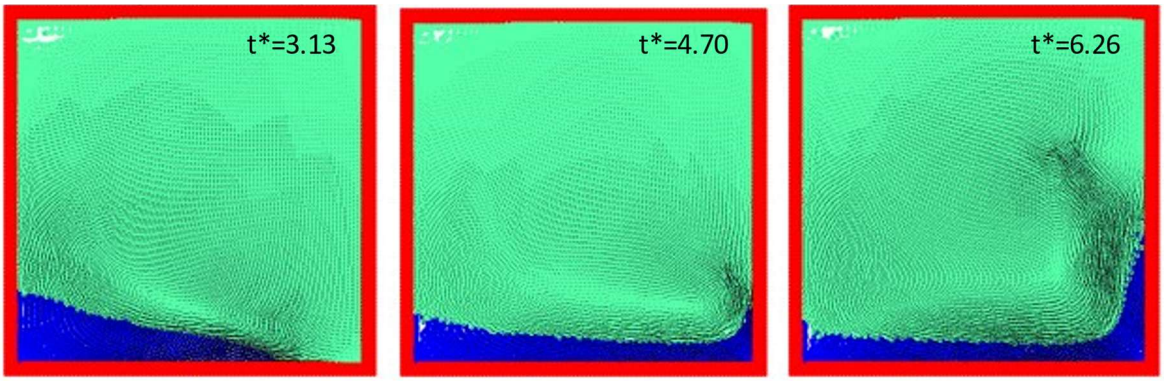

Figure 3.2 Calculation results of water column collapse in gas

Figure 3.2 shows the calculation results for the density ratios of 1/1000 and 1/10.

Here, $t^* = t\sqrt{\left({}^{2g}/_{L}\right)}$ The gas around the water creates a vortex above the collapsing water column as shown in Figure 3.3.

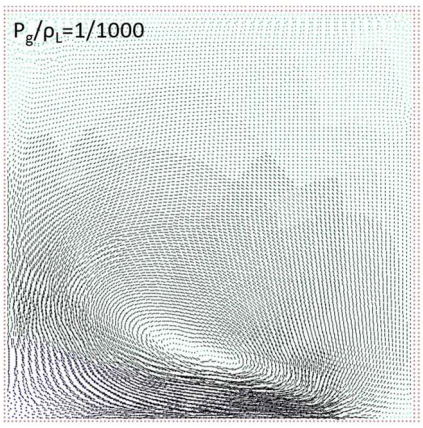

Figure 3.3 Vector representation of flow in gas water column collapse at t*=3.13

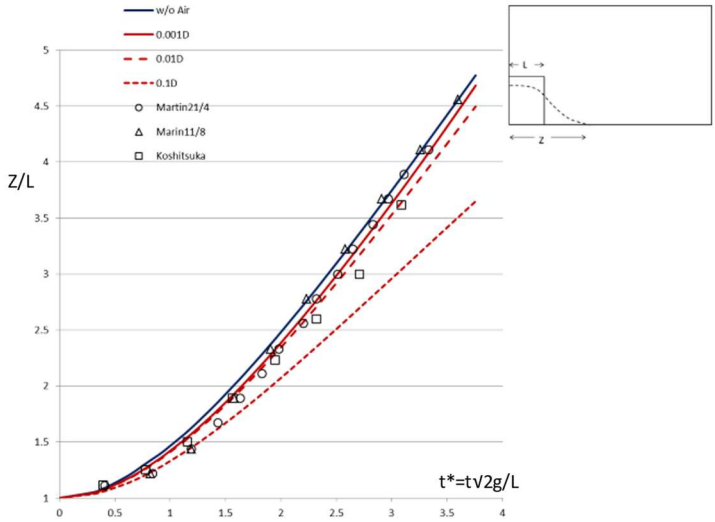

Figure 3.4 Changes in the tip position in the calculation of water column collapse in gas

Figure 3.4 shows the time change of the tip position of the collapsed water column. Experimental data is also shown. The calculation result without considering the gas has a slightly faster tip speed than the experimental data. The calculation result of the density ratio 1/1000 is also slightly faster than the experimental data. When the density ratio is increased, the change in tip speed is small in the case of a density ratio of 1/100, but when it becomes about 1/10, the tip speed clearly slows down.

3.2 2D Bubble Rising Analyses

Analysis of a bubble rising in water is often taken up as a typical subject of gas-liquid two-phase flow. Figure 3.5 shows the analysis system for a bubble rising in the water. The bubble

/ water density ratio is 1/1000. When a single bubble rises in water by buoyancy, surface tension, viscosity, and inertial force determine the bubble behavior. Since the experimental results of this bubble behavior are summarized by Grace[3], the analysis conditions are plotted in Grace's diagram as shown in Figure 3.6. Mo, Bo and Re are defined as follow:

$$Mo = {g\mu^4}/{\rho\sigma^3} \qquad (15)$$

$$Bo = {gd^2\rho}/{\sigma} \qquad (16)$$

$$Re = \left({Bo^3}/{Mo}\right)^{\frac{1}{4}} \qquad (17)$$

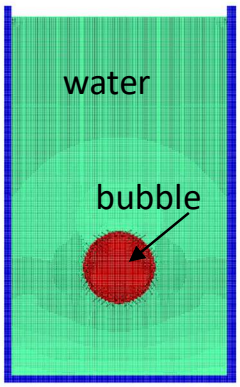

Case 1	Case 2
Mo=2.58×10^{-11}	Mo=2.58×10^{-11}
Bo=212.8	Bo=53.2
Re=24800	Re=8766
R=20mm	R=10mm

Figure 3.5 Analysis system of bubbles rising in water

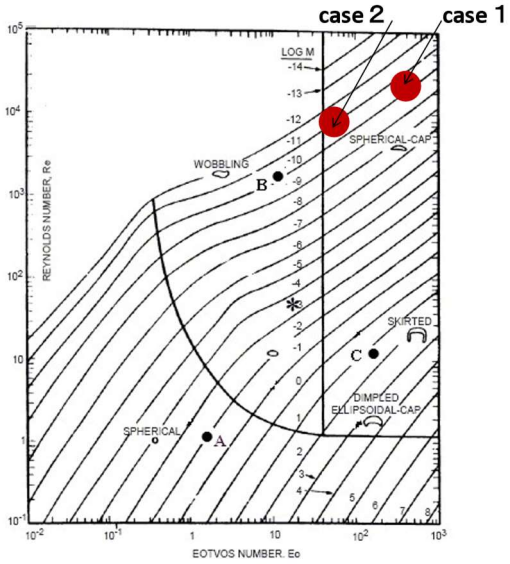

Figure 3.6 Explanation of analysis case by Grace's experimental data

According to the figure, it is expected that the case 1 will be a spherical cap and the case 2 will be a spheroid. The calculation result of Case 1 is shown in Figure 3.7. Here, the dimensionless time t * is $t^* = t\sqrt{\left({g}/{R}\right)}$, where R is bubble radius. The bubble shape is close to the spherical cap as epected. The calculation result of Case 2 is shown in Figure 3.8.

The shape of the bubble is similar to that of a spheroid as expected by the Grace chart.

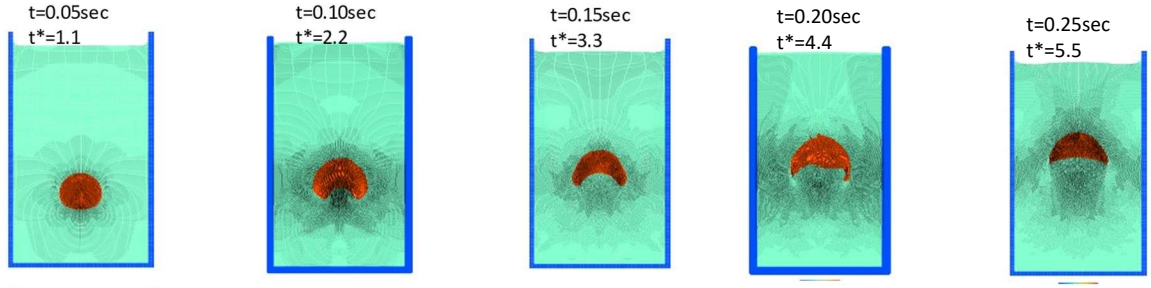

Figure 3.7 Analysis result of case 1

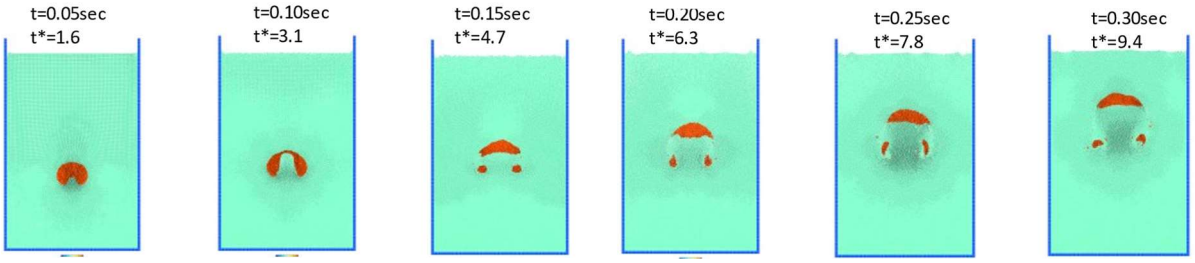

Figure 3.8 Analysis result of case 2

The bubble rising speed (terminal velocity) for cases 1 and 2 was almost the same as the experimental result [4] shown in Figure 3.9.

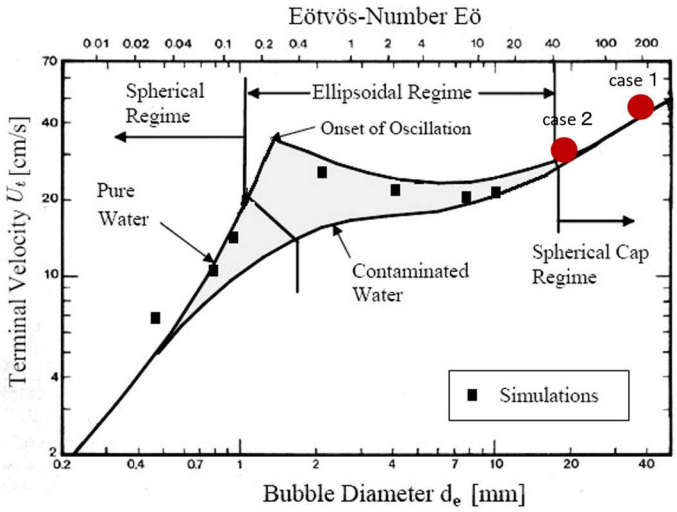

Figure 3.9 Results on the rate of bubble rise

3.3 2D Analyses of Gas Entrainment in Inclined Portion of Rectangular Cavity

A water test of vertical push-up from the bottom into a rectangular cavity on a 10 mm thick acrylic flat plate has been conducted[5]. In the experimental device (Figure 3.10 left), the rotary motion of the motor is changed to a vertical motion with a ball screw, and the piston is

moved at a constant speed to push the water in the cylinder into the cavity. The initial water level is set 50 mm below the bottom of the cavity.

The push-up speed is 1.0 and 2.0 m / sec. In the initial state, the cavity is filled with air at room temperature. Two vents are arranged at the top of the cavity. The filling of water in the cavity is video-recorded using a CCD camera. When the gate speed is 1.0 m / sec, the water that has passed through the gate will soon spread to the left and right, entraining gas at the bottom of the cavity and colliding with the side surface. After that, the filling proceeded while the central part of the cavity swelled. On the other hand, when the gate speed was 2.0 m / sec, the inflowing water rose vigorously while the tip part swelled and collided with the upper surface of the cavity. Entrained a large amount of gas. These tests were modeled as shown in Figure 3.10 and analyzed by the developed SPH method. The density ratio of gas to water is 1.2 / 1000. The distribution of flow velocity at the gate part seems to be the fastest in the center and the slowest in the part near the wall in the experiment, however in the analysis, the condition of constant flow velocity was given to the inlet part.

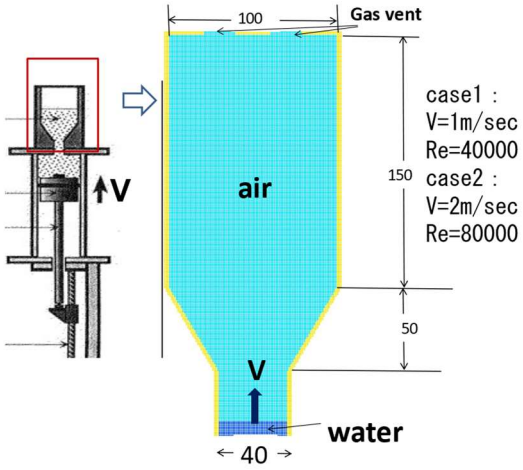

Figure 3.10 Experimental apparatus fof the vertical squeeze type casting and its analysis model

Figure 3.11 shows a comparison of the analysis and test results during the filling process for a push-up speed of 1.0 m / sec. The water gradually spreads laterally and rises to proceed with filling. Air remains in the channel expansion part (inclined part), and it can be seen that air is entrained at 0.16 sec in the test and at 0.24 sec in the analysis. The free surface shape is raised on both side walls, and the analysis well simulates the test results.

Figure 3.12 shows a comparison of the analysis and test results during the filling process for a push-up speed of 2.0 m / sec. The water rises slightly laterally and collides directly with the upper part of the cavity, and then fills the lower part along the outer circumference of the cavity. After the water collides with the upper cavity, the vent is closed. Therefore, no gas is emitted[5]. The analysis generally expresses the flow of the experiment. The analysis ended abnormally after 0.18 sec, because the vent was closed and the air particles were not discharged and consequently the number density of air particles increased abnormally.

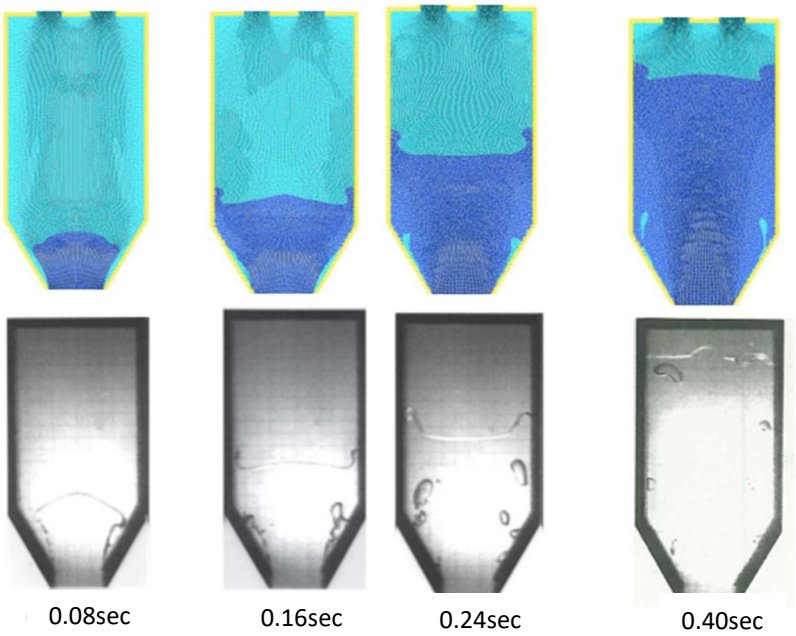

Figure 3.11 comparison of the analysis and test result for case 1

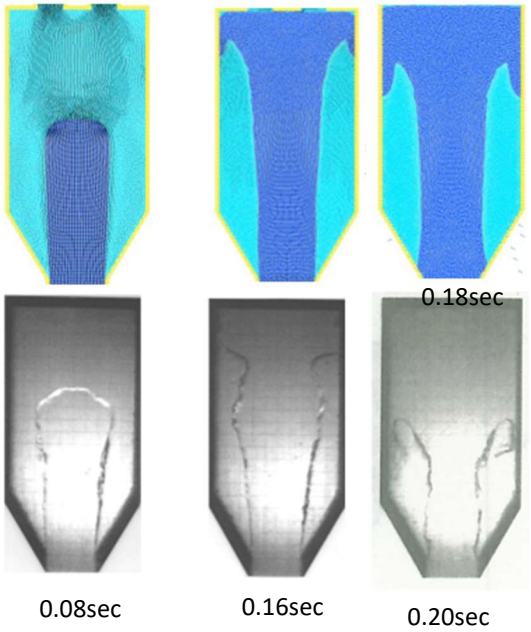

Figure 3.12 Comparison of the analysis and test result for case 2

3.4 2D Analysis of Air Exhaust from Backward Step Part of Die

A water model experiment has been conducted on the air exhaust behavior in the backward step part [6]. The experimental equipment (Figure 3.13 left) consists of a water tank ①, a direct acting 2-port valve ② and a test unit ③. The water in the tank pressurized by the air pressure from the compressor flows into the test section by opening the solenoid valve. The

test section (Figure 3.13, right) has a 20 mm thick transparent acrylic plate with a 2.0 mm deep groove and a flow path configuration that rapidly expands from a width of 15 mm to a width of 30 mm. A film sheet with a thickness of 0.02 mm is attached to the part other than the flow path. It has been reported over 7 cases of flow velocity, but since there is a photograph of the flow condition in the case of u = 8.41 m / sec, this was analyzed. The velocity u is defined as a value obtained by dividing the water discharge amount by the cross-sectional area of the width 15 mm × the thickness 2.02 mm at the entrance of the test section. If the corresponding Re is defined by the step of 15 mm in the enlarged part, Re = 1.26×10^5 .

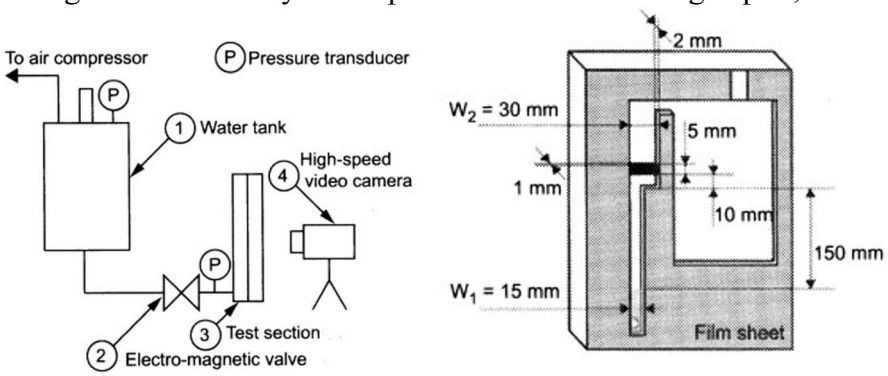

Figure 3.13 experimental equipment

Comparison of analysis results and experimental results [6] is shown in Figure 3.14 for each time. Here, the origin of time is the moment when the tip of the water flow enters the channel expansion portion. The analysis does not include the turbulent effect. At 12 ms in Figure (B), it collides with the downstream wall surface and flows to the right along the downstream wall surface. In Figure (C), it contacts the corner on the downstream right side of the channel expansion part at 22 ms in the experiment and 25 ms in the analysis. According to the literature, it is stated that "after that, a flowing upstream direction occurs along the enlarged flow path ", but in the analysis, the flowing upstream direction is extremely small. In Figure (D), there is a description that "a vortex containing bubbles is formed in the enlarged flow path". In the analysis, since the flowing upstream is small, only the vortex on the air side is conspicuous. In the literature, "then, as shown in Figures (E) and (F), the bubbles contained in the enlarged flow path are ejected into small bubbles due to the disturbance of the gas-liquid interface and gradually discharged. Most of the air is trapped in the enlarged flow path." Most of the air remains trapped in the enlarged part by the analysis too.

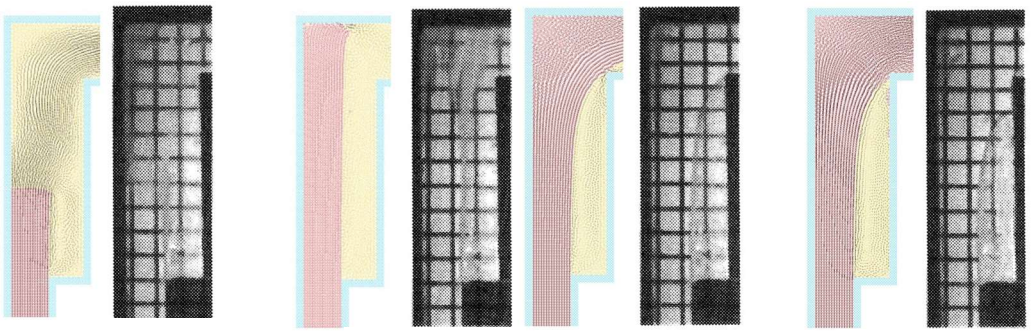

(A) 4ms (B) 12ms (C) 25ms(Analysis) 22ms(test) (D) 38ms

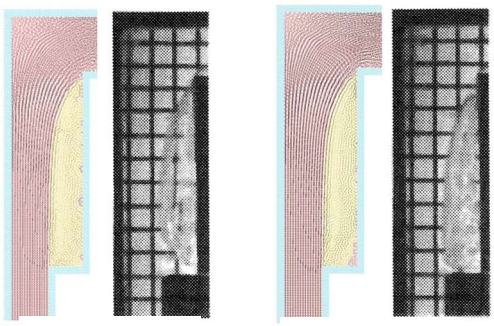

(E) 68ms (F) 118ms

Figure 3.14 Comparison of analysis results and experimental results

3.5 3D Bubble Rising Analysis

A three-dimensional analysis of a bubble rising in water was performed. Figure3.15 shows the comparison between two-dimensional analysis model and three dimensional one. Since 3D analysis requires a lot of calculation time, the analysis area is limited compared to 2D. The bubble / water density ratio was 1/1000. Figure 3.16 shows the calculation results for the bubble radius R = 10 mm together with the two-dimensional results. Here, $t^* = t\sqrt{(g/R)}$. The bubble shape at the time of rising became similar to a spheroid as shown in the experimental result summarized by Grace[3].

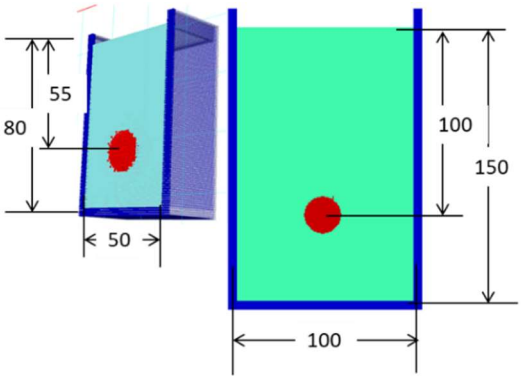

Figure 3.15 3D model and 2D model

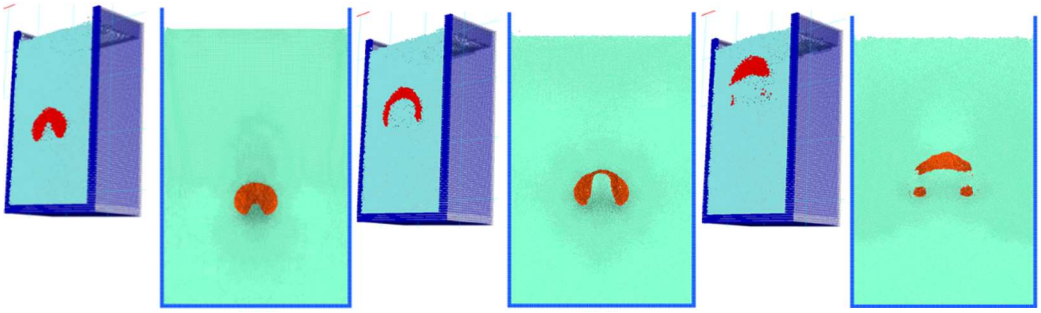

t=0.05sec, t*=1.6 t=0.10sec, t*=3.2 t=0.15sec, t*=4.7

Figure 3.16 Calculation results for the bubble radius R = 10 mm

4 ANALYSIS OF GAS ENTRAINMENT IN DIECAST

The mold filling process considering air entrainment in the die cast are simulated using the two-phase flow SPH method described in chapter **2**[7].

4.1 Analysis Model

The particle model that simplifies the 3D die-casting shape in the field is used in this simulation is shown in Figure 4.1.

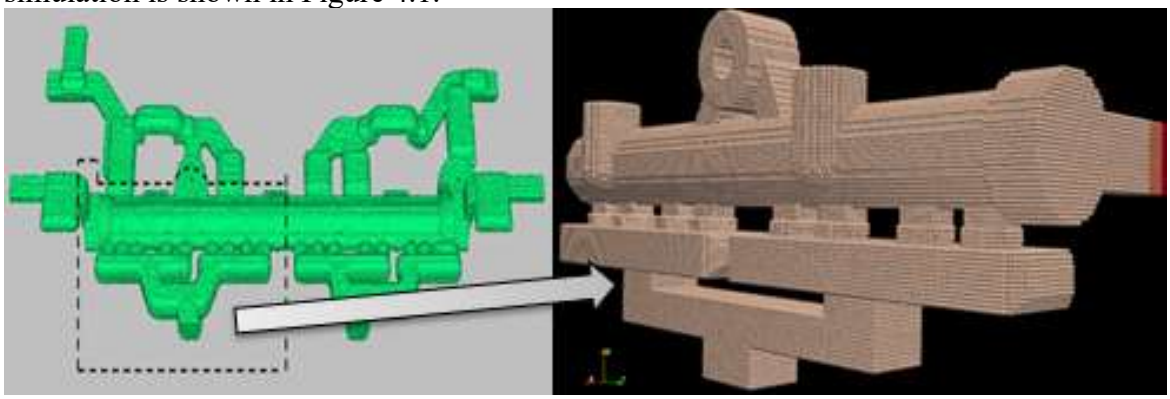

Figure 4.1 Analysis model for die casting

Total number of particles is 226,600, including initial air particles of 135,500. The particle length is 0.1cm. And particles with a specified speed flow in continuously at the molten metal inflow gate is shown in Figure 4.1 left.

4.2 Analysis Model

The material properties used in this simulation is shown in Table 4.1. The initial velocity of liquid Al alloy is 25m/sec and keeps constant during filling process.

Table4.1 Material Properties used for Analysis of Gas Entrainment in Diecast

Die-Cast	L=21.8cm, W=9.9cm, H=6.2cm, t=0.2cm	
Gas	Density	1.293Kg/m^3
	Kinematic Viscosity Coefficient	1.38x10^{-5}m^2/s
	Initial Pressure	1.013Pa
Liquid Al	Density	2500Kg/m^3
	Kinematic Viscousity Coefficient	1.0x10^{-6}m^2/s
	Surface Tension	0.9N/m
	Ingate Velocity	25m/s

4.3 Results

Figure 4.2 shows the results of the two-phase flow SPH simulation. it can be confirmed that from the start of injection, the liquid Al alloy splits to the left and right in the Die-Cast, the eight entrances pass through the narrow gate and flow toward the vent part and the several airs remain after the complete filling. The maximum flow velocity occurred at the gate.

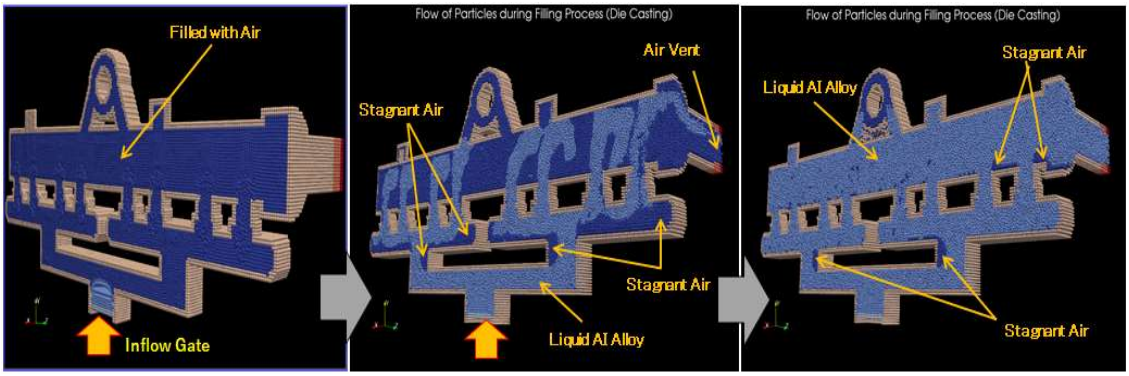

Figure 4.2 Analysis results of gas entraiment during die casting

5 CONCLUSIONS

- The gas-liquid two-phase flow was formulated using SPH.
- Authors analyzed several two-phase phenomina including the gas entrainment. All the analysis results are consistent with or similar to the test results.
- The developed methodology was applied to gas entrainment during the die cast filling process.

REFERENCES

[1] Hu, X. and Adams, N. A multi-phase SPH method for macroscopic and mesoscopic flows *J. Computational Physics* (2006) **213**: 844-861.

[2] Zhang, A, Sun, P. and Ming, F. An SPH modeling of bubble rising and coalescing in three dimensions. *Comp. Meth. in Applied Mech. and Engng*.(2015) **294**:189-209.

[3] Grace, Jr. Shapes and velocities of bubbles rising in infinite liquids. *Trans ICHemE* (1973) **51**:116-120

[4] Farhangi, M.M., Passandideh-Fard, M. and Bagherian B. Bubble rise and departure from a viscous liquid free surface. *Proc. IMECE2008*(2008) **68609**.

[5] Kanatani, R., Ohnaka, I., Zhu, Jin Dong and Kitamoto, S. Comparison Between Mold Filling Simulation Using Non-Orthogonal Element and Water Model Experiment. *J. Japan Foundry Engng* (1997) **69-3**:247-253.

[6] Ozaki, K, Fukuda, T., Nishi, A., Shimori, Y. and Hayakawa, T. Promotion of Air Exhaust from Backward Step Part of Die by Installing Rib by Using Flow Visualization Experiments with Water Flow. *JSME(A)* (2007) **73-726**: 99-104.

[7] Yamagata N. and Ichimiya M., Development of Mold Filling Process Simulation considering Air Entrainment using SPH Method, WCCM(2022) to be published.